

Noninnocent Ligands

Deutsche Ausgabe: DOI: 10.1002/ange.201510403
Internationale Ausgabe: DOI: 10.1002/anie.201510403

Delocalization and Valence Tautomerism in Vanadium Tris(iminosemiquinone) Complexes

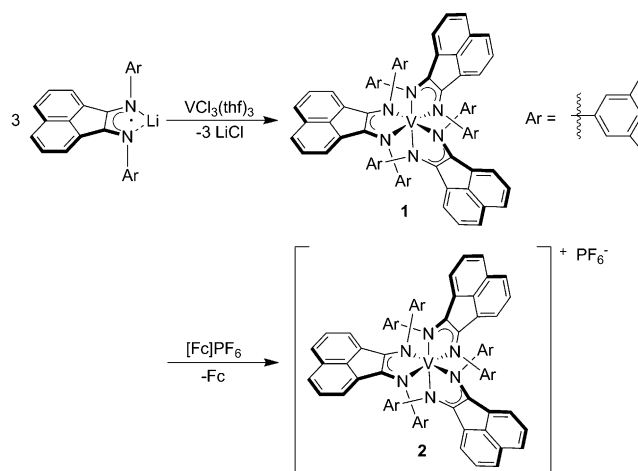
Jesper Bendix and Kensha Marie Clark*

Abstract: To survey the noninnocence of bis(arylimino)acenaphthene (BIAN) ligands (*L*) in complexes with early metals, the homoleptic vanadium complex, $[V(L)_3]$ (**1**), and its monocation, $[V(L)_3]PF_6$ (**2**), were synthesized. These complexes were found to have a very rich electronic behavior, whereby **1** displays strong electronic delocalization and **2** can be observed in unprecedented valence tautomeric forms. The oxidation states of the metal and ligand components in these complexes were assigned by using spectroscopic, crystallographic, and magnetic analyses. Complex **1** was identified as $[V^{IV}(L^{red})(L^{\cdot})_2]$ ($L^{red} = N,N'$ -bis(3,5-dimethylphenylamido)acenaphthylene; $L^{\cdot} = N,N'$ -bis(3,5-dimethylphenylimino)acenaphthenesemiquinonate). Complex **2** was determined to be $[V^V(L^{red})(L^{\cdot})_2]^+$ at $T < 150$ K and $[V^{IV}(L^{\cdot})_3]^+$ at $T > 150$ K. Cyclic voltammetry experiments reveal six quasi-reversible processes, thus indicating the potential of this metal–ligand combination in catalysis or materials applications.

Redox-active ligands represent an increasingly attractive and rapidly expanding class of ligands owing to their ability to act as electron reservoirs, thus providing unparalleled electronic stabilization of metal centers.^[1] In some cases, strong mixing of energetically similar ligand and metal frontier orbitals results in noninnocent behavior whereby the ascribed oxidation state assignment fails to describe the true charge distribution within the complex.^[2] In such cases, the resulting open-shell configurations generate complexes with unique electronic and magnetic properties that can be exploited for catalysis and materials applications.^[3] For more directed control over noninnocent behavior, it becomes necessary to elucidate the so-called spectroscopic oxidation state, which reflects the admixture of metal d orbitals and ligand frontier orbitals.^[2] Homoleptic complexes provide a path for extracting this information, as their high inherent symmetry facilitates electronic and structure treatments to provide parameters that can simplify analyses of more complex systems.^[4]

Recently, we reported the isolation of the neutral titanium tris(semiquinonate) complex, which was supported by the α -diimine ligand *N,N'*-bis(3,5-dimethylphenylimino)acenaphthenesemiquinonate (dmp-BIAN^{isq}; L^{\cdot}), and was found to not only undergo intramolecular electron transfer (IET), but also displayed unprecedented field-quenched, enhanced temperature-independent paramagnetism (TIP).^[5] This class of ligands are able to coordinate to metal centers in multiple oxidation states,^[6] and are known for electronic flexibility, including IET, with main-group,^[7] late transition,^[8] and f-block metals.^[9] Studies of the interactions between these ligands and early transition metals, however, are quite limited.^[10] As noninnocence is a function of both the redox-active ligand and the coordinated metal center,^[11] it was of interest to us to determine what effect, if any, changing the metal center would have on the electronic behaviour of an analogous tris(iminosemiquinonate) complex. Towards this goal, the neutral vanadium(III) complex, $[V(L)_3]$ (**1**), and its monocation, $[V(L)_3]PF_6$ (**2**), were synthesized and characterized.

Complex **1** was isolated in 59% yield from the reaction of $VCl_3(thf)_3$ and three equivalents of the anionic ligand, $Li[dmp-BIAN^{isq}]$ (Scheme 1). The monocation **2** was synthesized by the one-electron, chemical oxidation of **1** using $[Fe(C_5H_5)_2]PF_6$ ($[Fc]PF_6$) to afford **2** as dark green crystals in 76% yield (Scheme 1). The compositions of **1** and **2** were confirmed by elemental analysis and APCI mass spectrometry. While no 1H NMR signal was observed for **1**, paramagnetically broadened and shifted resonances for **2** were observed in $[D_8]THF$ (Figure SI1 in the Supporting Information). Varying the temperature between 190–338 K did not result in any significant changes in the spectrum.

Scheme 1. Syntheses of **1** and **2**.

[*] Dr. K. M. Clark

Department of Chemistry, University of California, Irvine
1102 Natural Sciences 2, Irvine, CA 92697 (USA)
E-mail: kmclark@uci.edu

Prof. J. Bendix

Department of Chemistry, University of Copenhagen
Universitets Parken 5, 2100 Copenhagen (Denmark)

Dr. K. M. Clark

Present address: Chevron Phillips Chemical Company, LP,
Building 94-E, PRC, Highway 60 & 123
Bartlesville, OK 74004 (USA)

Supporting information and ORCID(s) from the author(s) for this article are available on the WWW under <http://dx.doi.org/10.1002/anie.201510403>.

Single-crystal X-ray diffraction studies were conducted on **1** (Figure 1). This complex contains crystallographically imposed sixfold symmetry, which results in averaging of metrical parameters for the three ligands, making it difficult to distinguish the oxidation level (e.g. diamide, L^{red} ; diimino-semiquinonate, L^{\cdot} ; or diimine, L^{ox} ; Scheme 2) of each ligand

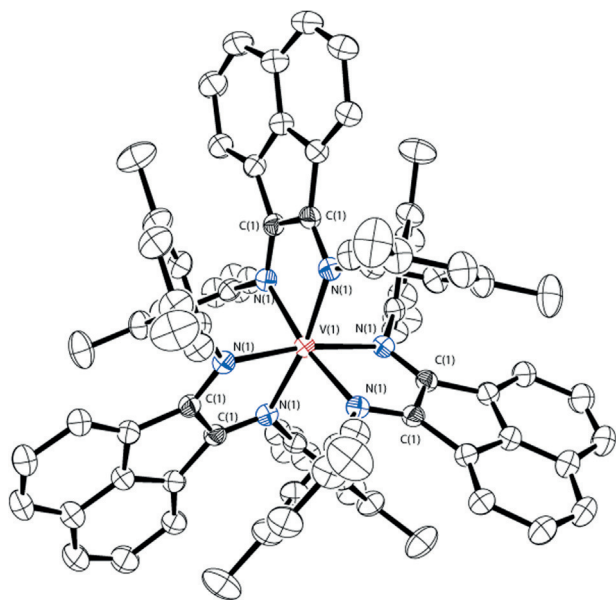
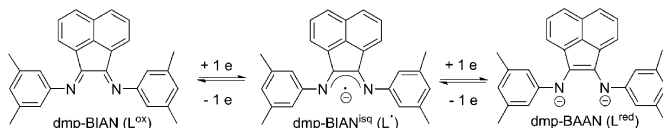


Figure 1. ORTEP diagram of $[V(C_{28}H_{24}N_2)_3] \cdot C_6H_6$ (**1**· C_6H_6) as determined by single-crystal X-ray diffraction studies. Thermal ellipsoids are shown at 50% probability. Hydrogen atoms and the solvent molecule have been omitted for clarity.



Scheme 2. First three oxidation levels of the BIAN ligand.

from these data. As expected, complex **1** was shown to possess local D_3 symmetry, whereby the six-coordinate titanium center is pseudooctahedral owing to a trigonal twist angle of 42° .^[12] The BIAN ligand has relatively small N–V–N ligand bite angles of $77.6(7)^\circ$ enforced by the five-membered chelate ring (V–N–C–C–N), and nearly linear *trans* N–V–N bond angles (ca. 171°), which is in good agreement with pseudooctahedral geometry. The average C–N_{Ar} bond length of **1** (ca. 1.33 \AA) is consistent with the value reported for the semiquinonate, $Na[dpp\text{-}BIAN^{\text{isq}}]$ (ca. 1.32 \AA) (dpp = 2,6-diisopropylphenyl).^[6] Furthermore, the C(1)–C(1) bond length was determined to be $1.436(3) \text{ \AA}$, a value that lies between that of the BIAN (ca. 1.47 \AA) and BAAN (ca. 1.39 \AA) oxidation levels.^[6]

X-band EPR spectra of complex **1** were collected in THF solutions at 77 and 298 K (Figure SI2). At 77 K, an eight-line spectrum centered at $g_{\text{iso}} = 1.998$ was observed. The hyperfine coupling constant, $A_i(^{51}\text{V}) = 92.3 \text{ G}$, which is larger than that typically observed for vanadium(IV) tris complexes (60–

80 G), indicates strong coupling of the electron to the vanadium nucleus (^{51}V , $I = 7/2$, 99.8%).^[13] The hyperfine couplings to the six equivalent nitrogen nuclei were not resolved. Warming the sample to 298 K resulted in a loss of signal intensity, a g-factor shift to 2.003, and a decrease in the hyperfine coupling constant ($A_i(^{51}\text{V}) = 79.3 \text{ G}$). This illustrates that while the electron is still largely localized on the ^{51}V metal center, delocalization of electron density occurs with increasing temperature. These data suggest that, in the case of **1**, the oxidation state of the metal center is likely +4.

Solid-state magnetism data for **1** was collected in the range of 5–300 K (Figure 2). This complex exhibits a doublet ground state, $S = 1/2$ ($\mu_{\text{eff}} = 1.69 \mu_B$ at 5 K) with μ_{eff} values

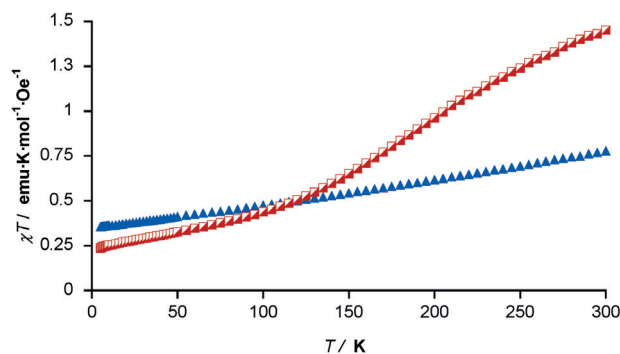


Figure 2. Plot of χT versus temperature, T , for **1** (blue) and **2** (red).

increasing with temperature, thus suggesting the presence of close-lying, thermally accessible excited states. Furthermore, the χT value increases linearly with T , which is consistent with TIP behavior; however, the observed TIP is an order of magnitude larger than expected for 3d systems.^[14] This magnetic behavior implies the occurrence of strong antiferromagnetic coupling between the vanadium metal center and the ligand radicals, which is countered by coupling between ligand radicals to result in yield spin frustration. The local vanadium zero field splittings complicate the picture, as does the trigonal symmetry and concomitant orbital degeneracy of the complex, which introduces Jahn–Teller instability that lowers the energy of its $S = 3/2$ vibronically coupled components to produce thermally accessible, close-lying excited states.^[15]

The absorption spectrum of complex **1** contains a series of intervalence charge transfer (IVCT), ligand to ligand charge transfer (LLCT), and interligand charge transfer (ILCT) bands in the near-infrared (NIR) and visible regions at 1430 nm ($\epsilon = 8510 \text{ M}^{-1} \text{ cm}^{-1}$), 890 nm ($\epsilon = 22300 \text{ M}^{-1} \text{ cm}^{-1}$), 620 nm ($\epsilon = 9300 \text{ M}^{-1} \text{ cm}^{-1}$), 560 nm ($\epsilon = 8700 \text{ M}^{-1} \text{ cm}^{-1}$), and 472 nm ($\epsilon = 2790 \text{ M}^{-1} \text{ cm}^{-1}$) (Figure SI3). These absorption peaks indicate both electronic delocalization and the presence of semiquinone ligands.^[16] An intense, presumably, LMCT transition is observed at $\lambda_{\text{max}} = 326 \text{ nm}$ ($\epsilon = 37500 \text{ M}^{-1} \text{ cm}^{-1}$).

Whilst X-ray diffractometry studies confirm that three dmp-BIAN ligands chelate the metal center, specific diagnostic information beyond the presence of reduced ligand oxidation state(s) cannot be extracted. Spectroscopic and magnetic analyses, however, provide evidence for specific ligand

and metal oxidation states. Namely, at 5 K, an $S = 1/2$ ground state was observed for **1**, which has magnetic behaviour that is indicative of TIP only, meaning the metal and ligands in complex **1** maintain the same oxidation state throughout the temperature range 5–300 K. Considering the EPR spectra observed for **1** almost unequivocally suggest a V^{4+} metal center, the most likely metal-ligand configuration is $[V^{IV}-(L^{\text{red}})(L^{\text{red}})_2]$, whereby the $S = 1/2$ metal center is ligated by one dianionic L^{red} ligand ($S = 0$), and two antiferromagnetically coupled L^{red} ligands ($S = 1/2$). This ligand arrangement is supported by the presence of IVCT and LLCT bands in the electronic spectrum. Furthermore, the magnetism and electronic spectra for **1** indicate this complex is a class III mixed-valence species according to the Robin–Day classification scheme.^[17]

The monocation **2** displays markedly different behaviour to **1**. As previously mentioned, a ^1H NMR spectrum was observed for **2**, whilst no signal was observed for **1**. Conversely, EPR spectra were recorded for **1**, and no signal was observed for **2**. Even more prominent are the differences in magnetic behaviour in the 5–300 K temperature region for **1** and **2**, whereby **1** displays only TIP and **2** exhibits a broad spin transition at about 150 K (Figure 2). Interestingly, for **2**, the μ_{eff} at 5 K is $1.33 \mu_B$, which indicates the presence of antiferromagnetic coupling. After the spin transition occurs, the μ_{eff} value increases to approximately $3.41 \mu_B$. This change is diagnostic of the uncoupling of electronic spins, and indicates that **2** exists as temperature-dependent valence tautomers (class II mixed-valences species).^[17] This phenomenon, to the best of our knowledge, is the first reported example with vanadium.^[18]

Taking into consideration the magnetic behaviour of **2**, the crystal structure was determined at 100, 153, and 250 K. Similar to **1**, the structure of **2** at each temperature contains crystallographically imposed sixfold symmetry. The overall local geometry about the vanadium remains pseudooctahedral with D_3 symmetry, independent of temperature changes (Figure 3); however, inspection of the bond angles highlights several small changes (Table 1). At 100 and 153 K, the bond angles in the vanadium coordination sphere linger within error of each other, having *trans* N–V–N bond angles of approximately 171.9° and *cis* N–V–N bond angles alternating between approximately 95.5° and 90.4° . When the temperature is increased to 250 K, the *trans* N–V–N bond decreases by approximately 0.3° to 171.6° , and the *cis* N–V–N bond angles partially increase, alternating between around 96.0° and 90.4° about the *z*-axis. The N–V–N bite angle was also found to decrease to $77.98(8)^\circ$ from $78.41(8)^\circ$ at 100 K. Diagnostic changes were also observed in the intraligand and ligand–metal bond lengths.

Firstly, the diagnostic ligand C–NAr and C(1)–C(1) bond lengths at 100 K were found to be $1.324(2)$ and $1.446(4)$ Å, respectively. These values are unchanged from those of complex **1**, and suggest that the ligand oxidation states of **1** and those of **2** at 100 K are the same. The V–N bond length of **2** at 100 K ($2.0505(15)$ Å) is shorter than that of **1**, thus indicating a smaller vanadium ionic radius. When the temperature of **2** is raised to 250 K, this bond becomes elongated by around 0.016 Å to $2.0666(16)$ Å. This elongation implies that

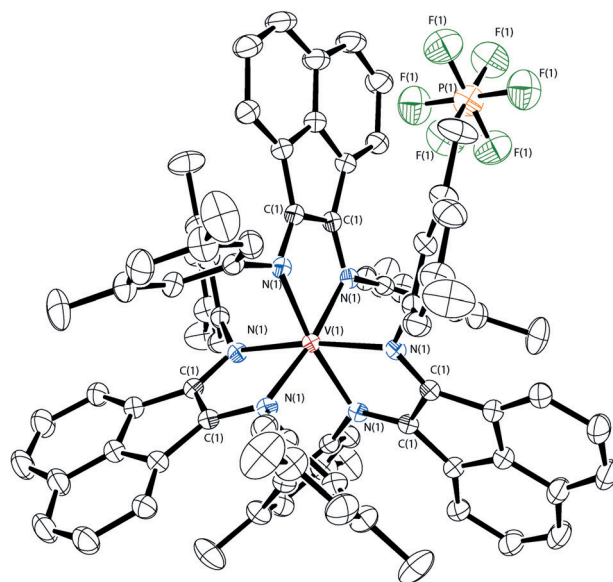


Figure 3. ORTEP of $[V(C_{28}H_{24}N_2)_3]PF_6$ (**2**) as determined by single-crystal X-ray diffraction studies at 153 K. Thermal ellipsoids are shown at 50% probability. Hydrogen atoms have been omitted for clarity.

Table 1: Selected bond lengths [Å] and angles [$^\circ$] for **1** and **2**.

	1 ·C ₆ H ₆	2 ^[a]	2 ^[b]	2 ^[c]
V–N(1)	2.0660(13)	2.0505(15)	2.0498(12)	2.0666(16)
C(1)–N(1)	1.323(2)	1.324(2)	1.3188(19)	1.313(2)
C(1)–C(1)	1.435(3)	1.446(4)	1.445(3)	1.445(3)
N(1)–V–N(1)	77.61(7)	78.41(8)	78.35(7)	77.98(9)
N(1) _{eq} –V–N(1) _{eq}	91.64(7)	90.39(8)	90.31(7)	90.41(8)
N(1) _{ax} –V–N(1) _{ax}	170.55(7)	171.95(8)	171.97(7)	171.66(9)
N(1) _{ax} –V–N(1) _{eq}	95.72(5)	95.86(5)	95.93(5)	96.08(6)

[a] $T = 100$ K. [b] $T = 153$ K. [c] $T = 250$ K.

the vanadium metal center has been reduced at high temperatures. It is noteworthy that this bond length is the same as that determined for **1**, which is proposed to be a vanadium(IV) complex. Furthermore, this change is accompanied by a contraction of the C–NAr bond lengths to $1.313(2)$ Å, thus suggesting one of the three BIAN ligands has been oxidized.

The NIR spectrum of cation, **2** (Figure S13), contains an intense transition at 1916 nm ($\epsilon = 18700 \text{ M}^{-1} \text{ cm}^{-1}$), that is followed by a broad transition at 930–1200 nm ($\epsilon = 14400 \text{ M}^{-1} \text{ cm}^{-1}$), which presumably arise from overlapping IVCT and LLCT bands.^[14] In the visible region, a series of IL transitions at 690 nm ($\epsilon = 8020 \text{ M}^{-1} \text{ cm}^{-1}$), 610 nm ($\epsilon = 5920 \text{ M}^{-1} \text{ cm}^{-1}$), and 510 nm ($\epsilon = 6850 \text{ M}^{-1} \text{ cm}^{-1}$) similar to **1** are observed. There are two additional, likely, LMCT bands observed at 404 nm ($\epsilon = 12800 \text{ M}^{-1} \text{ cm}^{-1}$) and 318 nm ($\epsilon = 45500 \text{ M}^{-1} \text{ cm}^{-1}$).

Electrochemical analysis of **1** and **2** by cyclic voltammetry at room temperature reveal virtually identical behavior, in which the two complexes undergo the same four quasi-reversible, one-electron redox processes; however, better solvent conditions resulted in a wider solvent window for **2**, thus allowing the observation of two additional reversible waves (Figure 4). The six reversible one-electron waves occur at -3.62 V, -2.65 V, -1.97 V, -1.07 V, -0.68 V, and $+0.46$ V

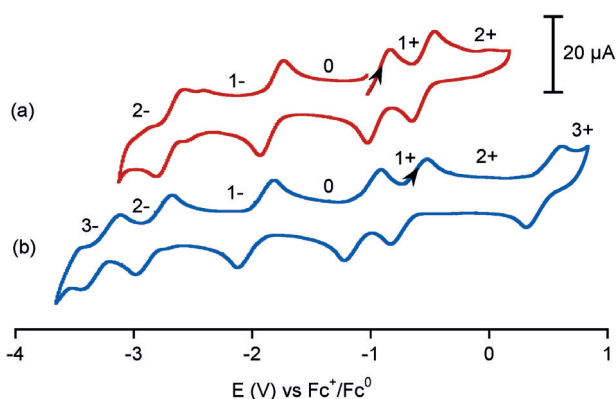


Figure 4. Cyclic voltammograms in THF (0.10 M $[t\text{Bu}_4\text{N}]\text{PF}_6$) of a) **1** and b) **2** at a glassy carbon working electrode and a scan rate of 200 mV s^{-1} .

versus the Fc^+/Fc couple for **2**. Similarities between the peak potentials of **1** and **2** with those reported for the analogous titanium complex^[5a] indicate these processes occur at orbitals with significant ligand character; however, the slightly positive shift of the vanadium complexes suggests that the HOMOs of **1** and **2** are lower in energy than that of the titanium derivative. The events at -0.68 V and $+0.46 \text{ V}$ represent the $[\text{V}(\text{L}_3)]^{2+}/[\text{V}(\text{L}_3)]^+$ and the $[\text{V}(\text{L}_3)]^{3+}/[\text{V}(\text{L}_3)]^{2+}$ couples, respectively, while the processes at -1.07 V , -1.97 V , -2.65 V , and -3.62 V are assigned to the $[\text{V}(\text{L}_3)]^0/[\text{V}(\text{L}_3)]^+$, $[\text{V}(\text{L}_3)]^0/[\text{V}(\text{L}_3)]^-$, $[\text{V}(\text{L}_3)]^+/[\text{V}(\text{L}_3)]^{2-}$, and $[\text{V}(\text{L}_3)]^{2-}/[\text{V}(\text{L}_3)]^{3-}$ couples, respectively.

These data unambiguously illustrate the changes in oxidation state associated with the monocation **2**. The presence of $^1\text{H NMR}$ resonances and the absence of an EPR signal strongly suggest an even spin system. Furthermore, magnetism data are consistent with an $S=0$ ground state arising from weak antiferromagnetic coupling. The transition to $S=1$ at high temperatures is corroborated by changes in intraligand and ligand–metal bond lengths. These changes indicate that at low temperatures, the ligand configuration is identical to that of **1**, and the only difference is the vanadium oxidation state. When the temperature is increased, an electron is transferred from a ligand to the metal center. These data confirm that at low temperatures the complex can be described as $[\text{V}^{\text{V}}(\text{L}^{\text{red}})(\text{L}')_2]^+$, which undergoes a spin transition with increasing temperature to become $[\text{V}^{\text{IV}}(\text{L}')_3]^+$. Interestingly, this assignment of the high-temperature valence tautomer is isostructural to the isoelectronic titanium analogue.^[5]

The similarities between these vanadium complexes and their titanium analogues lend further support to the conclusion that their observed electrochemical behaviour arises from molecular orbitals with significant ligand character. Based on this conclusion, we can identify the six species observed in the cyclic voltammogram as: $[\text{V}^{\text{IV}}(\text{L}^{3-})(\text{L}^{\text{red}})_2]^{3-}$, $[\text{V}^{\text{IV}}(\text{L}^{\text{red}})_3]^{2-}$, $[\text{V}^{\text{IV}}(\text{L}^{\text{red}})(\text{L}')_2]^-$, $[\text{V}^{\text{IV}}(\text{L}^{\text{red}})(\text{L}')_2]^0$, $[\text{V}^{\text{IV}}(\text{L}')_3]^+$, and $[\text{V}^{\text{IV}}(\text{L}^{\text{ox}})(\text{L}')_2]^{2+}$, where L^{3-} is the BIAN ligand radical trianion.^[6]

In summary, intramolecular charge redistribution is a property not uncommon amongst metal complexes con-

taining electroactive ligands; early metal complexes containing the redox-active BIAN ligand are no exception. Complex **1** was identified as $[\text{V}^{\text{IV}}(\text{L}^{\text{red}})(\text{L}')_2]^+$, a class III mixed-valence complex, whereby charge redistribution between ligands is nondiscrete. Two discrete redox isomers, $[\text{V}^{\text{V}}(\text{L}^{\text{red}})(\text{L}')_2]^+$ and $[\text{V}^{\text{IV}}(\text{L}')_3]^+$, were identified for **2**. This behavior represents a rare example of valence tautomerism in vanadium and further illustrates the relative noninnocence of the BIAN ligand system in complexes of early transition metals. Furthermore, the reversible nature of redox processes and the unusual magnetic behaviour in this system suggests strong potential for this metal–ligand combination in processes requiring the regeneration of oxidized or reduced species.

Acknowledgements

This research was funded by grants from the NSF (NSF CAREER Grant CHE-0645685) and conducted in part at UCI in the Heyduk Research Group. K.M.C. thanks the American–Scandinavian Foundation for financial support. We thank Dr. Joseph W. Ziller (University of California, Irvine) and Prof. Arnold Rheingold (University of California, San Diego) for the crystallographic data.

Keywords: mixed-valent compounds · noninnocent ligands · redox-active ligands · valence tautomerism · vanadium

How to cite: *Angew. Chem. Int. Ed.* **2016**, *55*, 2748–2752
Angew. Chem. **2016**, *128*, 2798–2802

- [1] a) W. Kaim, B. Schwederski, *Coord. Chem. Rev.* **2010**, *254*, 1580–1588; b) C. G. Pierpont, C. W. Lange, *Prog. Inorg. Chem.* **1994**, *41*, 381–492.
- [2] P. Chaudhuri, C. N. Verani, E. Bill, E. Bothe, T. Weyhermüller, K. Wieghardt, *J. Am. Chem. Soc.* **2001**, *123*, 2213–2223.
- [3] a) E. Coronado, J. R. Galán-Mascarós, C. J. Gómez-García, V. Laukhin, *Nature* **2000**, *408*, 447–449; b) S. C. Bart, E. Lobkovsky, P. J. Chirik, *J. Am. Chem. Soc.* **2004**, *126*, 13794–13807.
- [4] a) A. I. Poddol'sky, V. K. Cherkasov, G. A. Abakumov, *Coord. Chem. Rev.* **2009**, *253*, 291–324; b) C. G. Pierpont, *Coord. Chem. Rev.* **2001**, *219*, 415–433; c) C. G. Pierpont, *Inorg. Chem.* **2011**, *50*, 9766–9772.
- [5] K. M. Clark, J. Bendix, A. F. Heyduk, J. W. Ziller, *Inorg. Chem.* **2012**, *51*, 7457–7459.
- [6] I. L. Fedushkin, A. A. Skatova, V. A. Chudakova, G. K. Fukin, *Angew. Chem. Int. Ed.* **2003**, *42*, 3294–3298; *Angew. Chem.* **2003**, *115*, 3416–3420.
- [7] N. J. Hill, I. Vargas-Baca, A. H. Cowley, *Dalton Trans.* **2009**, 240.
- [8] D. J. Tempel, L. K. Johnson, R. L. Huff, P. S. White, M. J. Brookhart, *J. Am. Chem. Soc.* **2000**, *122*, 6686–6700.
- [9] a) I. L. Fedushkin, O. V. Maslova, E. V. Baranov, A. S. Shavyrin, *Inorg. Chem.* **2009**, *48*, 2355–2357; b) I. L. Fedushkin, O. V. Maslova, M. Hummert, H. Schumann, *Inorg. Chem.* **2010**, *49*, 2901–2910; c) I. L. Fedushkin, O. V. Maslova, A. G. Morozov, S. Dechert, S. Demeshko, F. Meyer, *Angew. Chem. Int. Ed.* **2012**, *51*, 10584–10587; *Angew. Chem.* **2012**, *124*, 10736–10739.
- [10] I. L. Fedushkin, V. M. Makarov, V. G. Sokolov, G. K. Fukin, M. O. Maslov, S. Y. Ketkova, *Russ. Chem. Bull.* **2014**, *63*, 870–882.
- [11] M. D. Ward, J. A. McCleverty, *J. Chem. Soc. Dalton Trans.* **2002**, 275–288.
- [12] P. Zanello, M. Corsini, *Coord. Chem. Rev.* **2006**, *250*, 2000–2022.

- [13] C. G. Pierpont, S. Kitigawa in *Inorganic Chromotropism: Basic Concepts and Applications of Colored Materials* (Ed: Y. Fukada), Springer, Berlin, **2007**, pp. 116–135.
- [14] O. Kahn, *Molecular Magnetism*, VCH Publishers, New York, **1993**.
- [15] B. Tsukerblat, A. Tarantul, A. Müller, *J. Mol. Struct.* **2007**, 838, 124–132.
- [16] D. Herebian, E. Bothe, F. Neese, T. Weyhermüller, K. J. Wieghardt, *J. Am. Chem. Soc.* **2003**, 125, 9116–9128.
- [17] M. B. Robin, P. Day, *Adv. Inorg. Chem. Radiochem.* **1967**, 9, 247–422.
- [18] a) D. N. Hendrickson, C. G. Pierpont, *Top. Curr. Chem.* **2004**, 234, 63–95; b) T. Tezgerevska, K. G. Alley, C. Boskovic, *Coord. Chem. Rev.* **2014**, 268, 23–40.

Received: November 9, 2015

Revised: January 7, 2016

Published online: January 22, 2016